The Abdus Salam
International Centre for Theoretical Physics

United Nations
Educational, Scientific and
Cultural Organization

IAEA
International Atomic Energy Agency

2152-24

Joint ICTP-IAEA Course on Natural Circulation Phenomena and Passive Safety Systems in Advanced Water Cooled Reactors

17 - 21 May 2010

EXPERIMENTAL VALIDATION AND DATA BASE OF SIMPLE LOOP FACILITIES

P.K. Vijayan and A.K. Nayak
Reactor Engineering Division
Bhabha Atomic Research Centre Trombay
Mumbai
India

IAEA Training Course on Natural Circulation Phenomena and Passive Safety Systems in Advanced Water-Cooled Reactors, ICTP, Trieste, Italy, 17-21 May 2010

Lecture Notes for T-15

on

EXPERIMENTAL VALIDATION AND DATA BASE OF SIMPLE LOOP FACILITIES

by

P.K. Vijayan and A.K. Nayak

Reactor Engineering Division, Bhabha Atomic Research Centre
Trombay, Mumbai-400085, INDIA

May 2010

EXPERIMENTAL VALIDATION AND DATA BASE OF SIMPLE LOOP FACILITIES

P.K. Vijayan[1] and A.K. Nayak[2]
Reactor Engineering Division, Bhabha Atomic Research Centre, Trombay, Mumbai 400085, India

1: E-mail: vijayanp@barc.gov.in
2: E-mail: arunths@barc.gov.in

KEY WORDS

Conditionally stable, Hysteresis, stability map, Limit cycles, Chaos

LECTURE OBJECTIVES

Industrial NCSs are quite complex in geometry and as such the phenomena taking place is not easy to understand and hence simple loop facilities are found to be useful in phenomena tracking. This lecture will highlight the contribution of simple loop facilities in improving our understanding of the steady state, transient and stability behaviour of NCSs.

1. INTRODUCTION

Simple loops are easier to construct and operate, require a minimum of instrumentation and large amount of easily reproducible data can be generated in less time at a very low cost. The greatest advantage of simple loop facilities is that the phenomena taking place is easily traceable and hence they are well suited for phenomenological investigations. Above all, theoretical and computational modelling of simple loops is far easier and less time consuming. Consequently, experiments in simple loop facilities have contributed greatly to improve our understanding of the natural circulation process. Besides, the experimental data from simple loop facilities have been useful in theoretical model development, computer code development as well as validation and phenomena identification. Both single-phase and two-phase natural circulation have been studied extensively in simple loop facilities, and the topics of investigation included steady state, transient and stability behaviour, development and testing of scaling laws, effect of operating procedures on the stability threshold, etc. Other favourite topics with experimentalists include parametric study of the effect of loop geometry, inventory variation, cold-water injection, start-up of NCSs, inception of boiling, parallel channel effects, effect of noncondensables, transition from forced to natural circulation, etc. Some notable contributions from simple loop experiments in the field of single-phase and two-phase NC are reviewed below.

2. STEADY STATE BEHAVIOUR OF SINGLE-PHASE LOOPS

Steady state flow prevails in a natural circulation loop when the driving buoyancy force is balanced by the retarding frictional force. The situation can be mathematically expressed as

$$-g\oint \rho dz = \frac{RW^2}{2\rho} \quad (1)$$

Where R is the total hydraulic resistance of the loop and is given by

$$R = \sum_{i=1}^{N} \left(\frac{fL}{D} + K \right)_i \frac{1}{A_i^2} \quad (2)$$

If we assume the Bossinesq approximation to be valid, then the density in the buoyancy force term can be expressed as

$$\rho = \rho_o \left[1 - \beta\left(T - T_0\right)\right] \quad (3)$$

Where ρ_0 is a reference density corresponding to the reference temperature T_0. Using this in Eq. (1), the steady state equation can be rewritten as

$$g\rho_0\beta \oint T dz = \frac{RW^2}{2\rho_0} \quad (4)$$

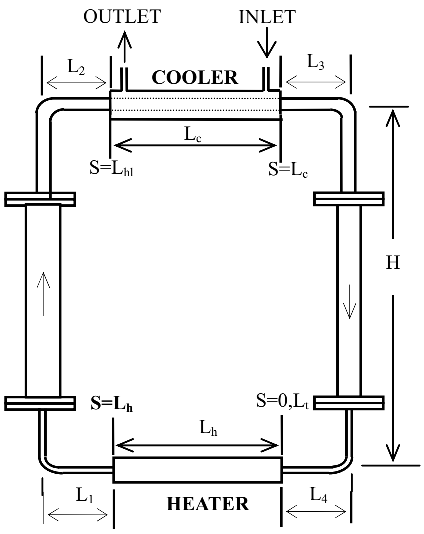

FIG. 1. NCL with horizontal heater and cooler

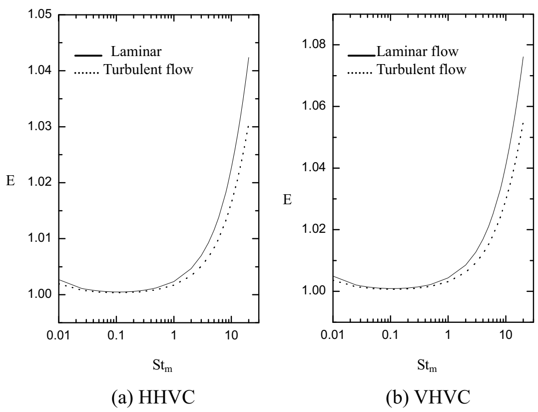

FIG..2.Error of approximation

Where the same reference density has been used to evaluate the loop hydraulic resistance. For a rectangular loop of height H with both cooler and the heater horizontal (Fig. 1), we obtain

$$g\rho_0\beta\left(T_{hl} - T_{cl}\right)H = \frac{RW^2}{2\rho} \quad (5)$$

The steady state temperature rise across the heater, ΔT_h can be expressed as

$$\Delta T_h = \frac{Q_h}{WCp} \quad (6)$$

Since $\Delta T_h = (T_{hl} - T_{cl})$, the steady state flow rate from Eq. (5) is obtained as

$$W = \left[\frac{2\rho_0^2 \beta g Q_h H}{RCp} \right]^{\frac{1}{3}} \tag{7}$$

Thus, we find that the steady state mass flow rate is proportional to the one-third power of the heater power. Many experimentalists used this equation to predict the natural circulation flow rate and compared with the measured flow (Zvirin (1981)). As the natural circulation flow rate in simple loops is too low to be accurately measured, it is usual to use the measured ΔT_h for comparison with data (Zvirin (1981)). By substituting the flow rate from Eq. (7) into Eq. (6), the ΔT_h at steady state can be estimated as

$$\Delta T_h = \left[\frac{RQ_h^2}{2\rho_0^2 \beta g H Cp^2} \right]^{\frac{1}{3}} \tag{8}$$

Thus the steady state temperature rise across the heater is found to be proportional to the two-third power of the heater power. It may be noted that both equations (7) and (8) are strictly valid for a rectangular loop with both the heater and cooler horizontal. However, other orientations of the heater and cooler are important to nuclear reactors. For example, in PWRs both the core and the steam generator (SG) are vertical whereas PHWRs have horizontal core and vertical SG and in VVERs, vertical core and horizontal SG is found. To account for the differences in orientation, often an additional assumption that the variation of temperature is linear in both the heater and cooler is used. With this assumption, the flow rate for any single-phase natural circulation loop can be obtained (Lewis (1977) or Todreas and Kazimi (1990)) as

$$W = \left[\frac{2\rho_0^2 \beta g Q_h \Delta Z_c}{RCp} \right]^{\frac{1}{3}} \tag{9}$$

Where ΔZ_c is the centre line elevation difference between the cooler and the heater. The above correlation was used to predict the flow rate in integral test loops for comparison with the measured values (Loomis and Soda (1982)). It may be noted that the problem with this approach is that the above equations are dimensional and it is not often possible to compare the performance of different natural circulation loops. For example, it is possible to obtain a larger flow rate in a loop with smaller height if its resistance is small. Therefore, search for a nondimensional equation for the steady state flow rate in natural circulation loops began. Today, it is possible to express the flow rate in a natural circulation loop in terms of generalized dimensionless groups (Vijayan (2002) and (2004)) if the local loss coefficient is replaced by an equivalent length, Le, such that

$$Le_i = \frac{K_i D_i}{f_i} \tag{10}$$

Thus, the effective length of the i^{th} segment can be expressed as

$$\left(L_{eff}\right)_i = L_i + Le_i \tag{11}$$

where the actual physical length is L_i. Using this, Eq. (4) can be recast as

$$g\rho_0\beta\oint Tdz = \frac{W^2}{2\rho_0}\left(\frac{fL_{eff}}{DA^2}\right)_i \tag{12}$$

Noting that the friction factor can be expressed by a correlation of the form

$$f_i = \frac{p}{\mathrm{Re}^b} \tag{13}$$

where p and b depend on the nature of the flow. For example, p=64 and b=1 for laminar flow and assuming the Blassius correlation to be valid for turbulent flow p and b are respectively 0.316 and 0.25. In a nonuniform diameter loop, it is possible that some pipe sections are in laminar flow, and some in turbulent flow and still others in transition flow. Even in uniform diameter loops, due to the differences in properties, the hot leg can be in the transition/turbulent region with the cold leg in the laminar region. However, if the entire loop is assumed to be either in laminar or in turbulent flow, then we obtain

$$\frac{2\rho_o^2\beta g Q_h H}{Cp} = p\mu^b W^{3-b}\sum_{i=1}^{N}\left(\frac{L_{eff}}{D^{1+b}A^{2-b}}\right)_i \tag{14}$$

For nonuniform diameter loops, we define a reference diameter and reference area as

$$D_r = \frac{1}{L_t}\sum_{i=1}^{N} D_i L_i \quad and \quad A_r = \frac{1}{L_t}\sum_{i=1}^{N} A_i L_i = \frac{V_t}{L_t} \tag{15}$$

where L_t is the total physical circulation length and V_t is the total loop volume. Using D_r, A_r and L_t to nondimensionalise the quantities in the bracket we obtain

$$\mathrm{Re} = \left[\frac{2}{p}\frac{Gr_m}{N_G}\right]^{\frac{1}{3-b}} = C\left(\frac{Gr_m}{N_G}\right)^r \tag{16}$$

$$\text{Where } N_G = \frac{L_t}{D_r}\sum_{i=1}^{N}\left(\frac{l_{eff}}{d^{1+b}a^{2-b}}\right)_i ; C = \left(\frac{2}{p}\right)^r \; and \; r = \left(\frac{1}{3-b}\right) \tag{17}$$

Thus, knowing the values of p and b the constants C and r can be evaluated. Eq. (16) is valid only for the case where both the heater and cooler are horizontal. With uniform heat flux, the actual temperature profile over the heater is linear. Similarly, the actual temperature profile in the primary side of the cooler is exponential. However, if we approximate it by a linear profile, then the generalized correlation valid for all orientations of the source and sink is given by

$$\mathrm{Re} = C\left[\frac{(Gr_m)_{\Delta z_c}}{N_G}\frac{H}{\Delta z_c} I_{ss}\right]^r \tag{18}$$

For the orientation with both the heater and cooler horizontal, we obtain I_{ss}=1, and H=Δz_c leading to

$$\mathrm{Re} = C\left[\frac{(Gr_m)_{\Delta z_c}}{N_G}\right]^r \qquad (19)$$

For other orientations of the source and sink, the same equation can be used if the error, E ($E=(H/\Delta Z_c)I_{ss}$), is small. For the case with uniform heat generation in the source, it is found that $I_{ss}=\Delta Z_c/H$ for the VHHC orientation leading to the same result as Eq. (19). For the HHVC and VHVC orientations, the calculations reported in Vijayan et al. (2004) shows that the error in using Eq. (19) is negligible (less than 1% if St_m is less than unity which is normally the case, see also Fig.2). Hence, the respective equations for a fully laminar and a fully turbulent loop can be obtained as

$$\mathrm{Re} = 0.1768\left[\frac{(Gr_m)_{\Delta z_c}}{N_G}\right]^{0.5} \qquad \text{Laminar loop} \qquad (20)$$

$$\mathrm{Re} = 1.96\left[\frac{(Gr_m)_{\Delta z_c}}{N_G}\right]^{\frac{1}{2.75}} \qquad \text{Turbulent loop} \qquad (21)$$

If part of the loop is in laminar or turbulent condition, then the above equations are not applicable. It may be possible to generate a correlation for part of the loop in laminar and part in turbulent flow. But if part of the loop is in laminar/turbulent flow with the rest in transition flow, then theoretical correlation is not possible due to the unavailability of friction factor correlation for the transition regime. However, it is possible to generate empirical correlations. One such correlation valid in the range $2\times10^8 < Gr_m < 10^{10}$ is given below (Vijayan et al. (1992))

$$\mathrm{Re} = 0.3548\left[\frac{(Gr_m)_{\Delta z_c}}{N_G}\right]^{0.43} \qquad (22)$$

For the special case of uniform diameter loops, $D_r=D$, $A_r=A$ so that $d_i=a_i=1$ leading to the following equation for N_G

$$N_G = \frac{L_t}{D}\sum_{i=1}^{N}\left(l_{eff}\right)_i = \frac{\left(L_{eff}\right)_t}{D}, \qquad (23)$$

so that $$\mathrm{Re} = C\left[(Gr_m)_{\Delta z_c}\frac{D}{\left(L_{eff}\right)_t}\right]^r. \qquad (24)$$

If the local losses are also negligible, then $N_G = L_t / D$ so that

$$\mathrm{Re} = C\left[(Gr_m)_{\Delta z_c}\frac{D}{L_t}\right]^r. \qquad (25)$$

2.1. Database for Uniform Diameter Loops (UDL)

The above correlations were extensively tested with data from simple loops. The loops considered included both uniform diameter loops (UDL) as well as nonuniform diameter loops (NDL). Among the simple uniform diameter loops, rectangular loops are experimentally studied most. Typical examples are the investigations by Holman and Boggs (1960), Huang and Zelaya (1988), Misale et al. (1991), Misale et al. (2007), Mousavian et al. (2004), Bernier and Baliga (1992), Vijayan et al. (1992), Hoe et al. (1997), Nishihara (1997) and Vijayan et al. (2001). Uniform diameter open loops were investigated by Bau-Torrance (1981) and Haware et al. (1983). Creveling et al. (1975) experimented with a uniform diameter toroidal loop. For all the UDL data covered in the present database, the loop diameter was in the range of 4 to 40 mm and the loop height varied from 0.38 to 2.3 m. The total circulation length varied from 1.2 to 7.2 m and the L_t/D ratio varied from 75 to 1100. The working fluid was mostly water and in one case Freon. The loop pressure was mostly near atmospheric except for the data of Holman and Boggs which was for near critical pressure. Database for all the four orientations of heater and cooler are included.

It was found that all UDL data neglecting the effect of local losses could be reasonably represented by the above generalized equation (Fig. 3). Effect of local losses was found to improve the agreement with the data in the turbulent regime (Vijayan (2002)). However, it has no significant influence in the laminar regime data since fL_t/D is much greater than sum of all loss coefficients.

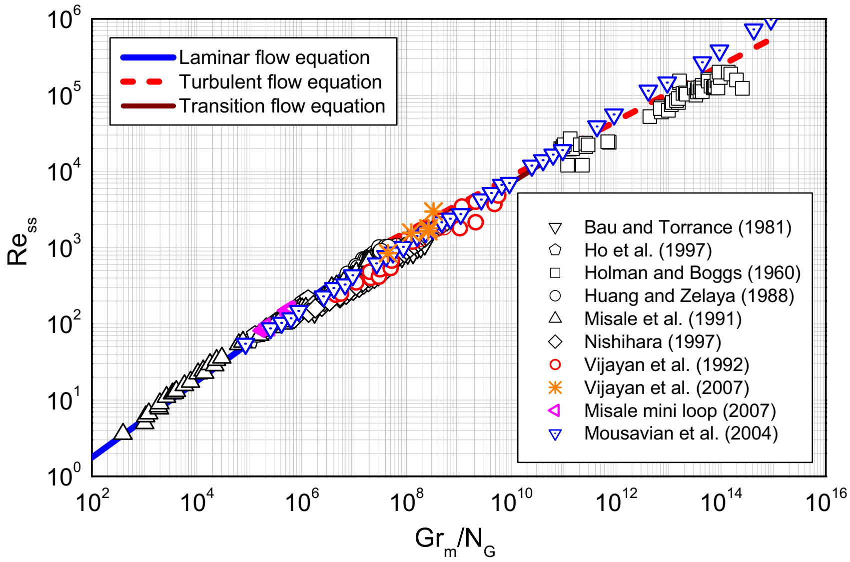

FIG. 3. Data from uniform diameter loops neglecting local losses

2.2. Database for Nonuniform Diameter Loops (NDLs)

Most practical applications of natural circulation employ non-uniform diameter loops. Common examples are the nuclear reactor loop, solar water heater, etc. Most test facilities simulating nuclear reactor loops also use non-uniform diameter loops. The non-uniform diameter loops experimentally studied can be categorized into two groups depending on the operating pressure as (1) High pressure loops and (2) Low pressure loops. Most studies are conducted in the high-pressure test facilities simulating nuclear reactor loops. Typical examples of such facilities are the SEMISCALE, LOBI, PKL, BETHSY, ROSA, RD-14 and FISBE. Some studies, however, are carried out in low pressure facilities. Examples are the experiments carried out by Zvirin et al. (1981), Jeuck et al. (1981), Hallinan-Viskanta (1986) Vijayan (1988), and John et al. (1991). Most of the available experimental data in a useable form (i.e. full geometrical details are known) are from the low-pressure test facilities. High-pressure test data in a useable form was available only from FISBE. The nonuniform loops considered had pipe segments with diameter varying from 3.6 mm to 97 mm and loop height varying from 1 to 26 m with pressure ranging from near atmospheric to 9 MPa. The total circulation length of the loops considered varied from about 10 to 125 m. All these loops used water as the working fluid. In-house as well as literature data on nonuniform diameter figure-of-eight loops are tested with the generalized equations. It also included the parallel-loops data of Jeuck et al. (1981) and Zvirin et al. (1981). The data from all NDLs are plotted in Fig. 4 neglecting the local losses.

Considering both UDL and NDL data, the low Reynolds number laminar (Re<350) and high Reynolds number turbulent (Re>10000) flow data show very good agreement with the respective theoretical correlations. For specific loops, good agreement with laminar flow correlation is observed even up to Re of 1200 and similarly turbulent flow correlation is found to give good results starting from Re > 2000. For the intermediate values of Gr_m/N_G ($2x10^6 < Gr_m/N_G < 10^{11}$) significant deviation is observed where the flow is neither fully laminar nor fully turbulent. Thus, it becomes clear that normal fully developed flow friction factor correlations are valid if the entire loop is either in laminar or turbulent flow irrespective of whether it is a UDL or NDL.

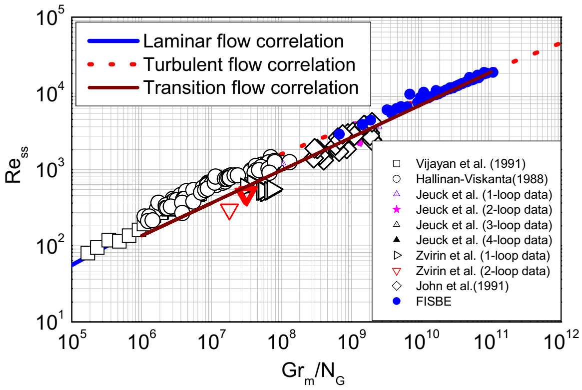

FIG. .4. NDL data neglecting local losses

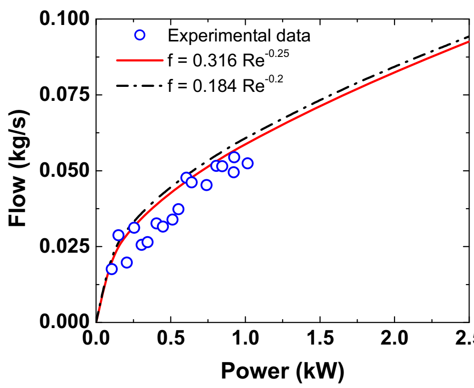

FIG. .5. All single-phase NC data neglecting local losses

Figures 5 and 6 show the effect of loop diameter on the steady state flow rate. As expected, the predicted single-phase flow is found to increase significantly with loop diameter (Fig.6).

3. STEADY STATE BEHAVIOUR OF TWO-PHASE LOOPS

One of the problems of two-phase natural circulation is that explicit equation for flow rate like Eq. (9) is not readily available even with homogeneous equilibrium model. However, it is possible to get approximate dimensional equation for flow rate (Dimmick et al. (2002) and Duffey (2000)). Todreas and Kazimi (1990) presents an equation for the steady state flow rate in a two-phase natural circulation loop relevant to a PWR. Rohatgi et al. (1998) obtained a dimensionless equation for the steady state condition neglecting the acceleration pressure drop. However, the dimensionless flow rate does not appear as a parameter in this equation. Assuming balance of the driving buoyancy force to the retarding frictional forces at steady state, Gartia et al. (2006) obtained the following equation for the steady state flow rate in a UDL.

$$W_{ss} = \left[\frac{2}{p} \frac{D^b \rho_l^2 \overline{\beta}_h g A^{2-b} Q_h \Delta z}{\mu_l^b N_G} \right]^{\frac{1}{3-b}} \qquad (26)$$

While deriving the above equation, they made an approximation equivalent to the Boussinesq in single-phase systems wherein the density in the buoyancy force term is expressed as $\rho = \rho_r[1-\beta_h(h - h_r)]$ with $\beta_h = (1/\mathrm{v})(\partial \mathrm{v}/\partial \mathrm{h})_p$. For frictional pressure loss estimation, ρ_l is used in the single-phase region. For the calculation of the frictional pressure loss in the heated two-phase and the adiabatic two-phase sections the two-phase friction factor multiplier, ϕ_{LO}^2, was used. The geometric number N_G is obtained as

$$N_G = \frac{L_t}{D_r}\left\{\sum_{i=1}^{N_{sp}}\left(\frac{l_{eff}}{d^{1+b}a^{2-b}}\right)_i + \overline{\phi}_{LO}^2 \sum_{i=N_{sp}+1}^{N_B}\left(\frac{l_{eff}}{d^{1+b}a^{2-b}}\right)_i + \phi_{LO}^2 \sum_{i=N_B+1}^{N_{tp}}\left(\frac{l_{eff}}{d^{1+b}a^{2-b}}\right)_i\right\} \qquad (27)$$

Gartia et al. (2006) showed that if Eq. (26) is expressed in dimensionless form would be same as Eq. (16) with Re *and* Gr_m defined as

$$\mathrm{Re} = \frac{D_r W_{ss}}{A_r \mu_l}; \; Gr_m = \frac{D_r^3 \rho_l^2 \overline{\beta}_h g Q_h \Delta z}{A_r \mu_l^3}$$

Fig. 7 shows a comparison of the measured flow rate with the theoretical equations for UDL and NDL. While plotting the data $\overline{\beta}_h = (\rho_{in} - \rho_e)/(\rho_m \Delta h_{ss})$ was used. In addition, the McAdams model was used to evaluate the two-phase friction factor. The steady state data used included four uniform diameter loops and two nonuniform diameter loops. The data falls in the following range of parameter: loop diameter: 9.1-99.2 mm, circulation length: 8.7-96.6 m, SD level: 90% $\pm$ 5%, pressure: 0.1-7 MPa, quality: 0.4-24%, inlet subcooling: 0.1-29K and power: 0.3-300 kW.

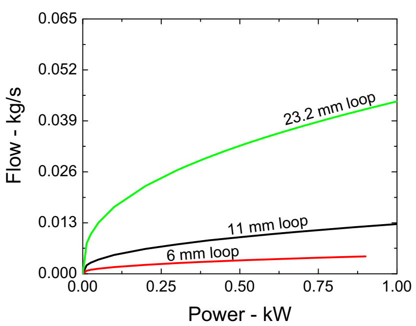

FIG. 6. Effect of loop diameter on predicted flow rate

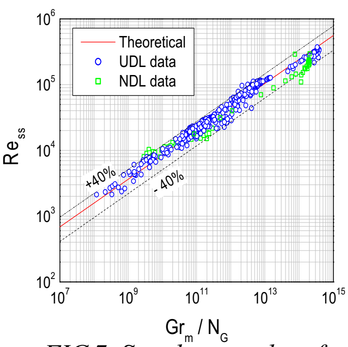

FIG.7. Steady state data from two-phase loops

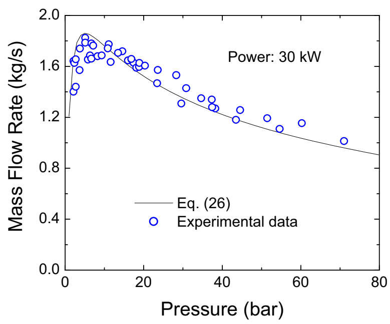

Fig.8: Effect of pressure on flow rate

Although, the equation was derived for the case without inlet subcooling, the data considered for testing included significant subcooling.

3.1 Parametric trends

One of the drawbacks of dimensionless correlations is that it often masks the parametric trends. In fact the steady state performance of two-phase loops is significantly influenced by the pressure, power and loop diameter. Effect of pressure on two-phase NC flow was studied experimentally and theoretically in the 49.3 mm i.d. loop and the results are shown in Fig. 8. The results are in agreement with the predictions of Eq. (26). The measured flow rate as a function of power is plotted in Fig. 9 for various loops. The predictions with Eq. (26), TINFLO-S (Nayak et al (2002)) and RELAP5/MOD3.2 are also given in Fig. 9. Again the data are in reasonable agreement with the predictions.

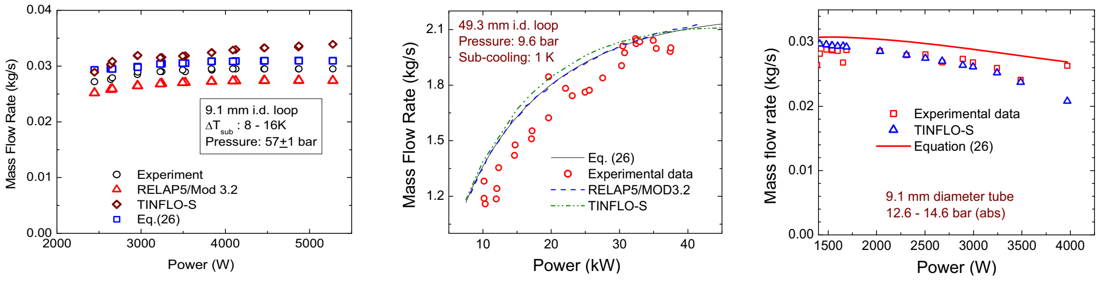

(a) (b) (c)

Fig.9: Effect of power on the two-phase NC flow rate

3.2 Two-phase NC Flow Regimes

Unlike single-phase natural circulation, it is observed that the trend of the steady state data can be significantly different for two-phase loops. Based on the nature of the variation of the steady state flow with power, three different natural circulation flow regimes can be observed for two-phase loops. These flow regimes are designated as gravity dominant, friction dominant and the compensating regimes. In a natural circulation loop, the gravitational pressure drop (being the driving pressure differential) is always the largest component of pressure drop and all other pressure drops (friction, acceleration and local) must balance the gravity (or buoyancy) pressure differential at steady state. However, the natural circulation flow regimes are differentiated based on the change of the pressure drop components with quality (or power).

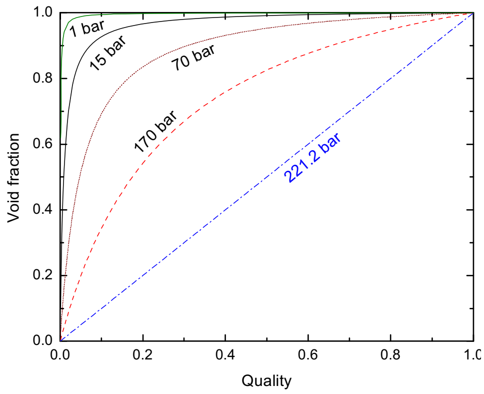

Fig.10: Effect of quality on void fraction

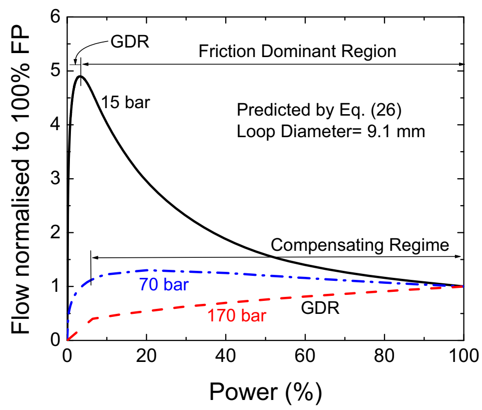

Fig. 11: Effect of pressure on flow regime

3.2.1 Gravity Dominant Regime

The gravity dominant regime is usually observed at low qualities. In this regime, for a small change in quality there is a large change in the void fraction (see Fig. 10) and hence the density and buoyancy force. The increased buoyancy driving force is to be balanced by a corresponding increase in the retarding frictional force that is possible only at a higher flow rate. As a result, the gravity dominant regime is characterized by an increase in the flow rate with power (compare Figs. 11 & 12 with Fig. 9b).

3.2.2 Friction Dominant Regime

Friction dominant regime is observed at low to moderate pressures when quality is high. At higher qualities and moderate pressures, the increase in void fraction with quality is marginal (Fig. 10) leading to almost constant buoyancy force. However, the continued conversion of high density water to low density steam at high qualities (due to the increase in power) requires that the mixture velocity must increase resulting in an increase in the frictional force and hence a decrease in flow rate. Thus the friction dominant regime is characterized by a decrease in flow rate with increase in power (see the curve for 15 bar in Fig. 11 and Fig. 9c).

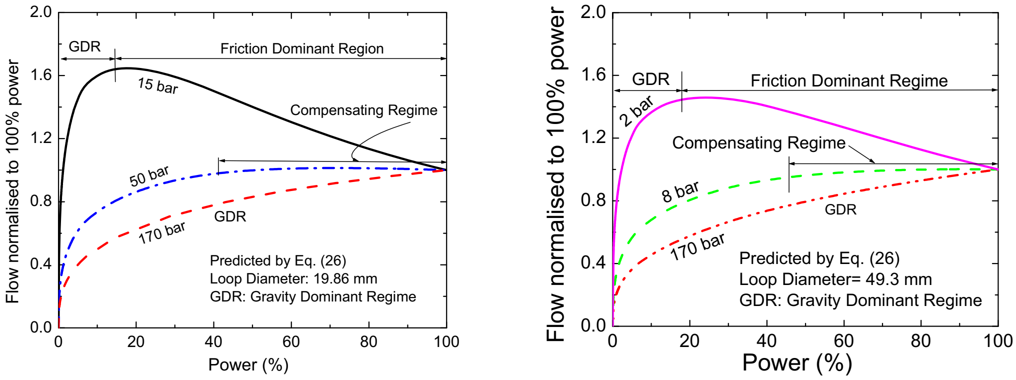

(a) (b)

Fig 12: Effect of pressure on flow regime for different loop diameter

3.2.3 Compensating Regime

Between the gravity dominant and friction dominant regimes, there exists a compensating regime, where the flow rate remains practically unaffected with increase in power. In this regime, the increase in buoyancy force is compensated by a corresponding increase in the frictional force leaving the flow unaffected (see Fig. 9a and the curve for 7 MPa in Fig. 11) in spite of increase in quality.

3.2.4 Effect of pressure and loop diameter

The NC flow regimes depend strongly on the system pressure. In fact, at high pressures only the gravity dominant regime (as in single-phase natural circulation) may be observed if the power is low. The friction dominant regime shifts to low pressures with increase in loop diameter (see Fig. 12). Knowledge of the flow regimes is important to understand the stability behaviour of two-phase loops.

4. STABILITY BEHAVIOUR OF SINGLE-PHASE LOOPS

Several investigators have carried out experimental investigations on the single-phase natural circulation instability. Examples are those by Creveling et al. (1975), Gorman et al. (1986), Widmann et al. (1989), Vijayan et al (1992), Nisihara (1997), Misale et al. (1998 & 1999), Satoh et al. (1998), Vijayan et al. (2001), Satou (2001), Jiang et al. (2002) and Vijayan et al. (2004). A few general characteristics of the oscillatory behaviour are brought out below

4.1. Conditionally Stable (Metastable or Hysteresis) Regime

Linear stability analysis tells us that the threshold of instability is a unique value for specified operating and geometric conditions. However, an important characteristic of the natural circulation instability is that the threshold of instability is not a unique value, but depends on the path followed in the experiment. For example, experiments in rectangular loops by Vijayan et al. (2001) showed that the instability thresholds are different for start-up from rest (Fig. 13), power raising from a stable steady state (Fig. 14) and power reduction from an unstable steady state (Fig. 15). The region in which the instability threshold shows path dependence is referred to as the conditionally stable or hysteresis regime. The region above the conditionally stable region is unconditionally unstable as it is always unstable independent of the heat addition path. Similarly the region below the lower limit of the conditionally stable region is unconditionally stable. Conditional stability (metastable or hysteresis region) is also found in systems with parallel channels (Chato (1963)) and in simple loops with a throughflow (Vijayan et al. (1992)). The hysteresis phenomenon is also observed in two-phase loops (Chen et al. (2001)).

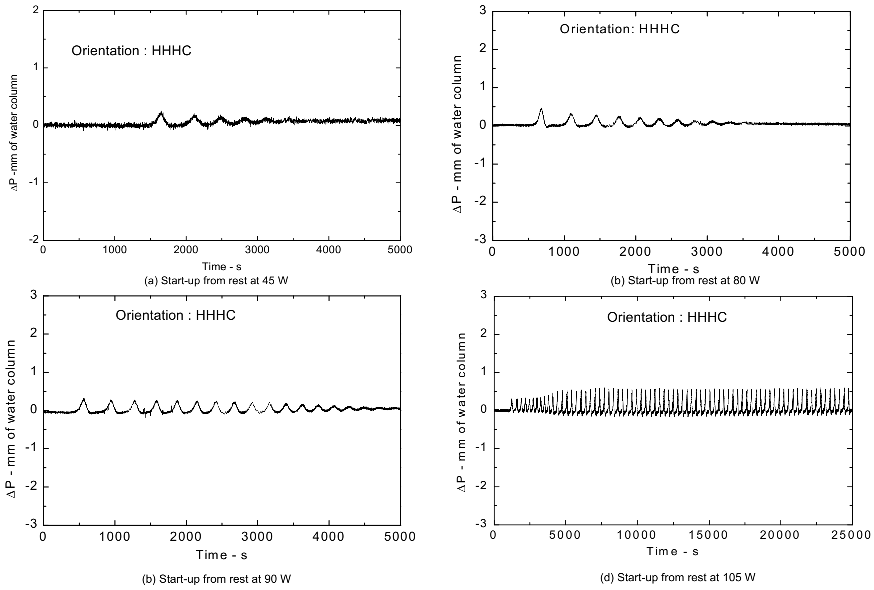

FIG. 13. Instability threshold for start-up from rest

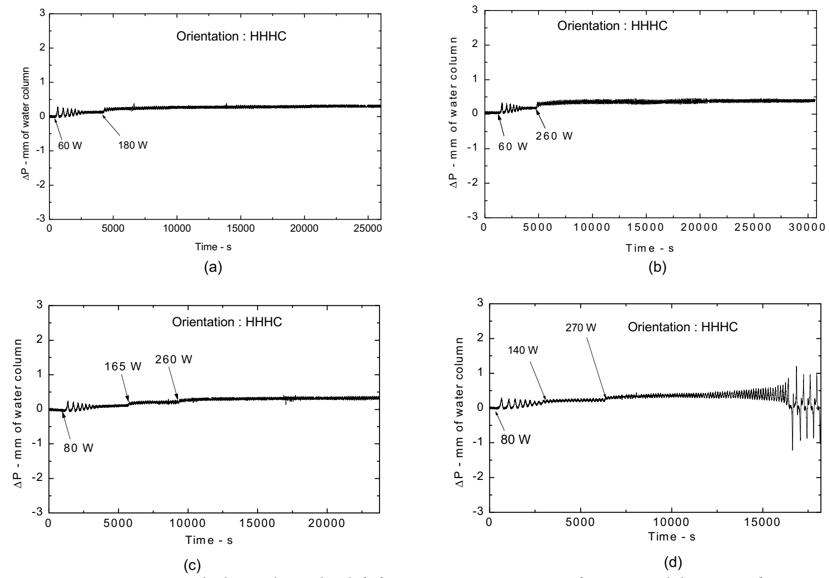

FIG. 14. Instability threshold for power raising from stable steady state

4.2. Mechanism causing instability and the Unstable flow Regimes

Based on numerical investigations in a rectangular loop with a point heat source at the bottom and a point heat sink at the top, Welander (1967) proposed that oscillation growth is the mechanism causing the instability. Available experimental data suggests that oscillation growth is indeed the mechanism causing instability (Fig. 16). However, subtle differences in oscillation growth can be seen from Fig. 16. Oscillation growth as proposed by Welander is always observed for the development of instability from the steady state case (Fig. 16a). For the case of start-up from rest, the oscillations are observed right from flow initiation (Fig. 16b & c) although an initial oscillation growth is visible. In all the three cases, the oscillation growth is terminated by the system nonlinearities leading to limit cycle oscillations with constant amplitude. In single-phase NC, the condition that the cooler outlet temperature on the primary side cannot be less than the secondary side coolant inlet temperature limits the minimum temperature. This together with the corresponding flow fixes the upper limit on heater outlet temperature as the heater power is fixed. The characteristics of the limit cycle oscillations observed are explained below.

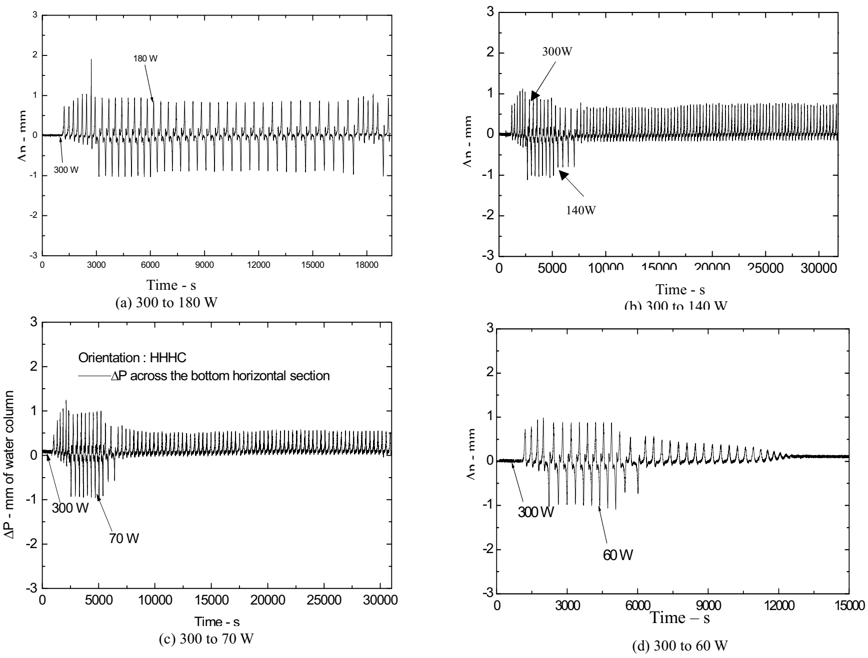

FIG. 15. Stability threshold for power reduction from an unstable state

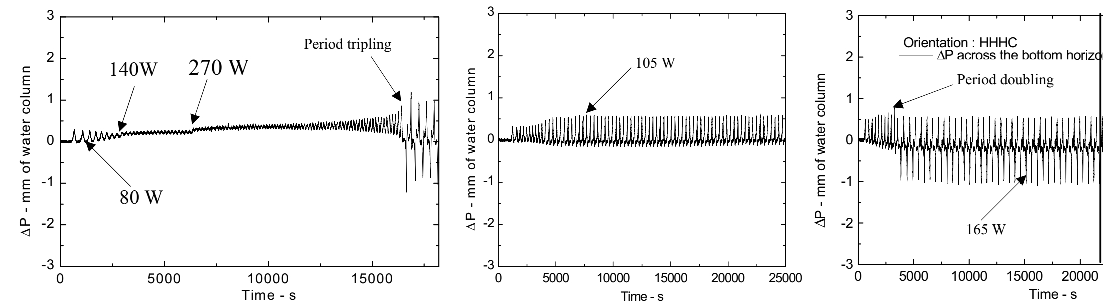

(a) Oscillation growth from steady state (b) Start-up from rest at low power (c) Start-up from rest at high power

FIG. 16. Development of instability through the oscillation growth mechanism

A qualitative difference in the limit cycle oscillations was observed at low and high powers. In the low power region, periodic unidirectional pulsing (UDP) as predicted by Keller (1966) was observed. Unidirectional pulsing portrays a bean shaped limit cycle in phase space (Fig. 17b). At high powers, periodic bi-directional pulsing (BDP) characterized by alternate forward and reverse flow is observed. Bi-directional pulsing portrays a double dumbbell shaped limit cycle in phase space (Fig. 17d).

Between these two, a regime where the oscillatory behavior switches from unidirectional to bi-directional pulsing in a chaotic manner is observed (Fig. 17e). Chaotic switching results in the spread around the dumbbell shaped phase trajectory as shown in Fig. 17f. With increase in power, the bi-directional pulsing regime continues but it becomes chaotic with each oscillation cycle depicting a distinct line resulting in the thick dumbbell shaped trajectory given in Fig. 17h. Long-term time series of unidirectional pulsing shows a characteristic comb like structure (Fig. 16b) whereas bi-directional pulsing shows a snake bone structure (Fig. 16c). In the short term, unidirectional pulsing appears to be repetitive flow initiations in the same direction whereas bi-directional pulsing is repetitive flow initiations in the opposite directions.

An interesting observation is that bi-directional pulsing flow regime alone is observed if power is raised from a stable steady state to an unstable value (Fig.18). Both the other flow regimes occur below the threshold power for this heat addition path. Unidirectional pulsing and chaotic switching, however, are observable both for start-up from rest (Fig. 13) and power step back from an initially unstable state (Fig. 15b and c).

Flow regimes observed in toroidal loops are much different from that observed in rectangular loops. For example, Gorman et al. (1986) observed three different chaotic regimes: a globally chaotic regime whose essential features can be described by a one-dimensional cusp-shaped map, a subcritical regime in which the flow can be either chaotic or steady, and a transient regime in which the flow remains chaotic for a time and then decays into a steady flow: The description of the subcritical regime appears to fit the conditionally stable regime observed in rectangular loops. However, periodic unidirectional oscillations were not observed in the toroidal loop (Creveling et al. (1975). Satou et al. (2001) report unidirectional oscillations, albeit in an inclined toroidal loop with a connecting tube.

4.3. Flow regime switching and oscillation period

Whenever the flow regime switches from unidirectional to bi-directional pulsing, the oscillation period enhances (Fig. 16c). On the other hand, when the flow regime switches from bi-directional to unidirectional pulsing, the oscillation period reduces (Fig 17e). Period doubling is a usual step for transition to chaos (Kapitaniak (2000)). Incidentally, the range of power where period doubling is observed is closely matching the observed chaotic switching regime. Beyond a critical value of power, chaotic switching is not observed. However, for start-up from rest flow initiates with unidirectional pulsing and then switches to bi-directional pulsing once (Fig. 15a and 16c). The period ratio for this first switching is found to be less than 2 and is found to decrease with increase in power. Tests carried out to check the repeatability of period ratio during flow regime switching, showed that the period ratio is reproducible within $\pm$ 8%. For switching from UDP to BDP following the small amplitude oscillation growth from an initial steady state, the period ratio can be significantly more than two (16a). However, there is no regular pattern in the observed period ratio and its value can be anywhere between 2 and 3.

4.4. Shape of the Limit cycle

The shape of the limit cycle depends on the chosen parameter space. Depending on the chosen parameter space, unidirectional pulsing can portray the jaws of a shark, the hood of a cobra, the sole of a shoe or a bean shaped limit cycle (Fig. 19). Similarly, bi-directional pulsing can portray a squirrel, a butterfly, a duck or a dumbbell (Fig. 20). Still, more shapes are possible with other parameter spaces.

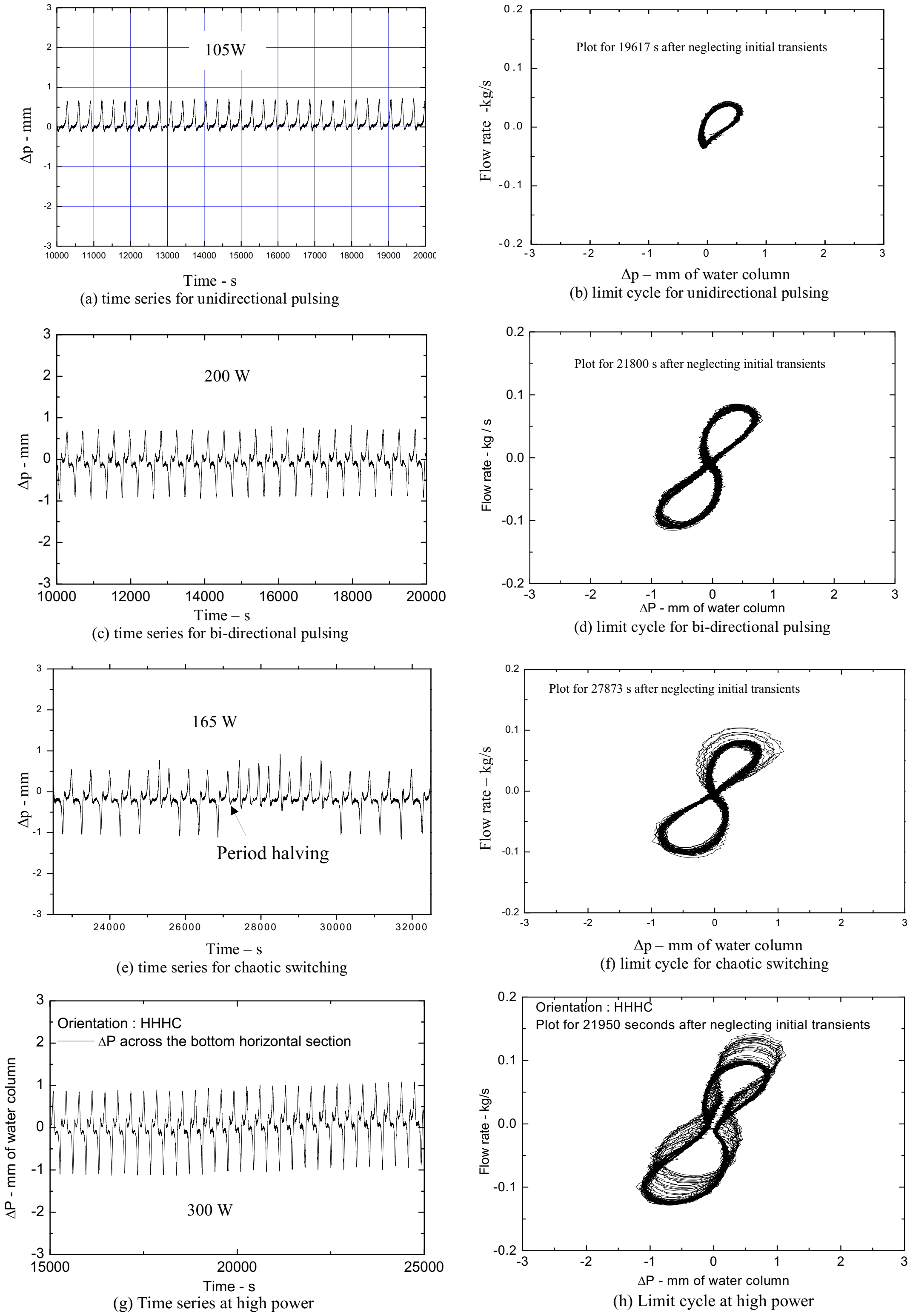

(a) time series for unidirectional pulsing

(b) limit cycle for unidirectional pulsing

(c) time series for bi-directional pulsing

(d) limit cycle for bi-directional pulsing

(e) time series for chaotic switching

(f) limit cycle for chaotic switching

(g) Time series at high power

(h) Limit cycle at high power

FIG. 17. Time series and limit cycles of unstable flow regimes in single-phase NC

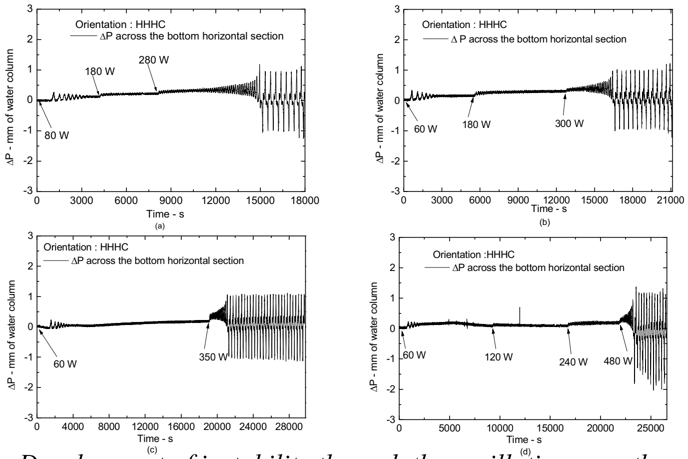

FIG. 18. Development of instability through the oscillation growth mechanism

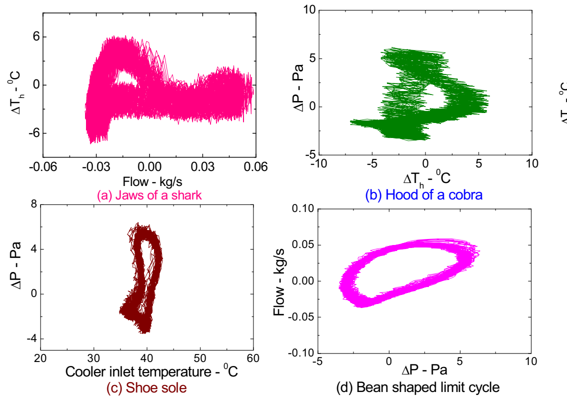

FIG. 19. Parametric effect on the phase plots for UDP at 140 W

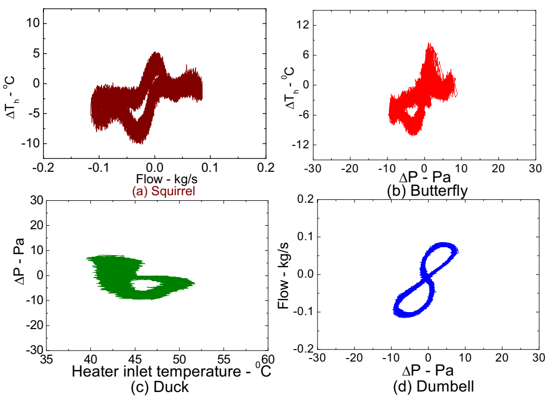

FIG. 20. Parametric effects on the limit cycle for BDP

4.5. Effect of power

The effect of power is to enhance the amplitude and frequency of the oscillations. Bi-directional pulsing is found to have considerably large period than unidirectional pulsing (Fig. 21). For unidirectional pulsing, the period decreases linearly with power whereas an exponential decrease is observed for bi-directional pulsing. As the power increases, the phase plots deform due to the occurrence of the higher oscillatory modes. At low power, the dumbbell just touches in the middle (Fig. 22) whereas it separates out at higher powers. Fig. 22 also shows that the bi-directional pulsing is somewhat aperiodic and the aperiodicity increases with power as is observed from the increased thickness of the phase plot. A 3-D phase plot showing the effect of power on the unstable flow regimes is shown in Fig. 23. The increase in amplitude with power results in the enhancement of the space enclosed by the limit cycles as seen in Fig. 23. The observed unstable flow regimes are also marked in this figure. A point in the phase space represents the stable steady state.

4.6. Prediction of the Stability Map

The stability map for single-phase NCSs is usually generated with the 1-D model neglecting the boundary wall effect. 1-D models show a very strong influence of the friction factor correlation on the stability threshold. Good comparison with experimental data can be obtained with a loop specific empirical correlation even though the theoretical model neglects the wall thermal capacitance, heat losses and 3-D effects (Creveling et al. (1975), Vijayan et al. (1992)). The same empirical correlation, when applied for other loops can show significantly different results. For example, Eq. (22) was found to predict the instability threshold of a 23.2 mm inside diameter rectangular loop reasonably well (Vijayan et al. (1992)). However, when the same correlation is used for the 26.9 mm inside diameter loop, the results are significantly different (Fig. 24). However, considering the heat losses and the thermal capacitance of the boundary walls, good prediction of the stability threshold can be expected for the fully laminar and fully turbulent loops. For certain geometric configurations such as that of the toroidal loop, the adequacy of the 1-D theory is questionable as the gravitational acceleration changes continuously over the loop.

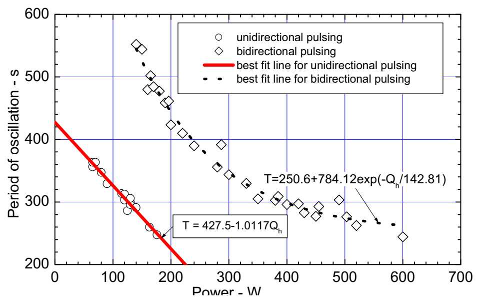

FIG. 21. Variation of oscillation period with power

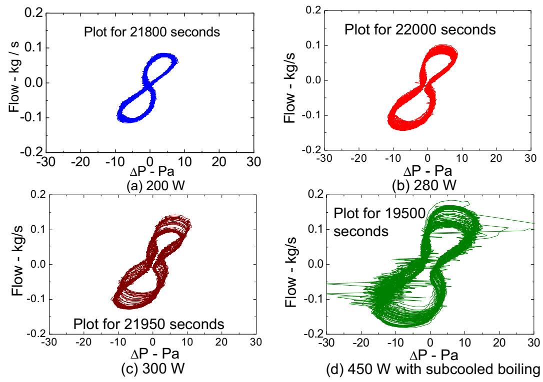

FIG. 22. Effect of power on BDP (plots neglect the initial transients)

4.7. Prediction of Limit Cycles

One dimensional theory using the fully developed friction factor and heat transfer correlations are found to be adequate for predicting the steady state behaviour of single-phase fully laminar and fully turbulent loops if the local pressure losses are also accounted. Good prediction of the stability map using the 1-D theory is expected for the fully laminar and fully turbulent loops if the thermal processes at the wall and the heat losses are accounted. However, predicting the limit cycle oscillations in natural circulation loops with repetitive flow reversals is a bigger challenge as all three (i.e. laminar, transition and turbulent) flow regimes can be encountered in the clockwise and anticlockwise directions in rapid succession in every oscillation cycle. In such cases, a criterion for laminar to turbulent flow transition is essential to be incorporated in the nonlinear codes. The transition criteria used are different in different codes (Vijayan et al. (1995) and Ambrosini et al. (2004)). Ambrosini et al. (2004) have shown that the use of an ad hoc friction correlation can lead to very interesting results like the appearance or disappearance of islands of stability. Prediction using the 1-D theory and the transition criterion described in Vijayan et al. (1995), the limit cycles predicted (Fig. 25) is found to be significantly different from the experimentally observed limit cycles (Vijayan et al. (2004)).

Due to the occurrence of laminar, transition and turbulent regimes with forward and reverse flow in every oscillation cycle (e.g. during oscillations with periodic flow reversals) the flow is never fully developed and the use of fully developed friction factor correlations and even the validity of the 1-D approximation itself is questionable for prediction of unstable flows. Use of multidimensional computer codes may be required for the prediction of the limit cycles.

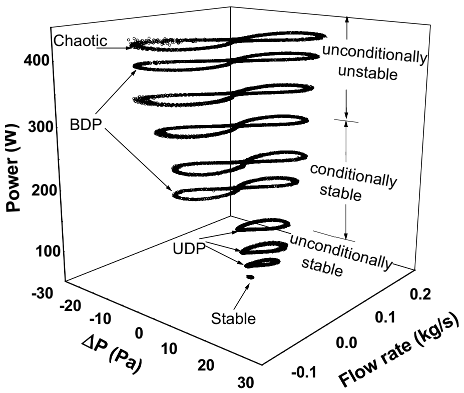

FIG. 23. 3-D phase space of instability (plot for 2500 seconds for each power neglecting the initial transients)

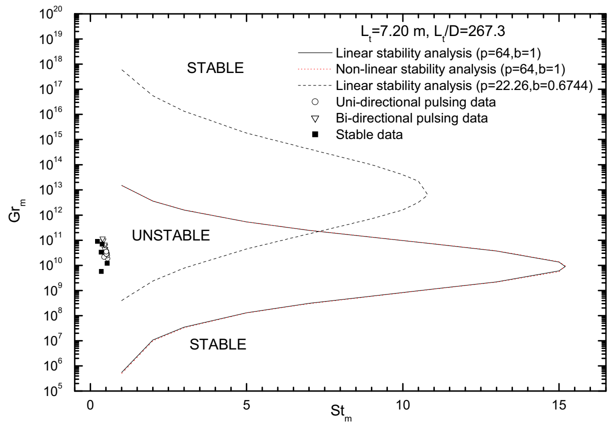

FIG. 24. Effect of friction correlations on the predicted stability map

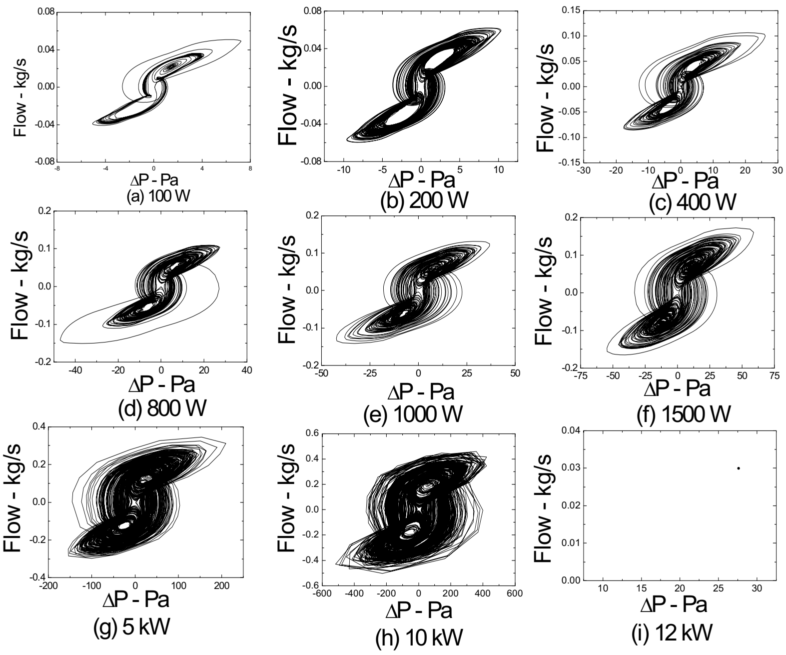

FIG. 25. Predicted limit cycles for different powers

4.8. Techniques for stabilizing

Knowledge of parametric trends helps us in avoiding instabilities. For example, VHVC (vertical heater vertical cooler) is found to be the most stable orientation of the source and sink in a rectangular loop. Hence, selection of this orientation is better for improving stability. The analysis results show that increasing the St_m and the L_t/D are ways of stabilizing. The latter option is more commonly used in natural circulation systems. In fact, single-phase instability is observed only for glass loops with $L_t/D < 300$. Increasing the length or decreasing the diameter will stabilise the loop. Misale et al. (1999) has used an orifice to stabilise single-phase NC flow. In single-phase flow, the location of the orifice does not play a significant role. However, one of the basic problems of orificing is that it reduces the flow rate significantly. Reduction in the flow rate results in the reduction of the heat transport capability of NC loops. However, there are several ways to stabilize NCSs without significantly reducing the flow rates. One of them is to use highly conducting or thick walled pipes for construction of the loop. Thick-walled tubes can diffuse the hot and cold pockets leading to stability (Misale (2000) and Jiang et al. (2002)). In addition, process control techniques can be used to stabilize the NC flow. These are beginning to be used in single-phase flow. For example, Fichera, and Pagano (2003) demonstrated the use of a proportional derivative control to stabilize single-phase NC instability.

5. EXPERIMENTAL DATABASE FOR INSTABILITY OF TWO-PHASE NC LOOPS

Extensive experimental database exist in literature for different kinds of flow instabilities which can occur in boiling two-phase natural circulation systems. Jain et al. (1966) conducted systematic investigations to find out the effects of various operating conditions such as heating power, subcooling, pressure, etc. on instability. Mostly, they observed the Type II density-wave instability in their experiments. Such behaviour was also observed in parallel heated channels of a two-phase natural circulation loop by Mathisen (1967). They observed density-wave instability in their experiments, which was found to increase with increase in channel exit restriction, inlet subcooling, and decrease in channel inlet restriction and downcomer level. Chexal and Bergles (1973) observed seven flow regimes when their loop was heated from cold condition, out of which three were steady and four were unstable. These regimes are (i) surface evaporation; (ii) a static instability characterized by periodic exit large bubble formation; (iii) a steady flow with continuous exit of small bubbles; (iv) a static instability characterized by periodic exit of small bubbles; (v) another static instability characterized by periodic extensive small bubble formation; (vi) a steady natural circulation; and (vii) the density-wave oscillation (dynamic instability). The static instabilities observed in their loop are due to the high heat flux and subcooled boiling occurring in the heated section, which are ideal for the chugging-type instability. Fukuda and Kobori (1979) observed two modes of oscillations in a natural circulation loop with parallel heated channels. One was the U-tube oscillation characterized by channel flows oscillating with 180^0 phase difference, and the other was the in-phase mode oscillations in which the channel flow oscillated along with the whole loop without any phase lag among them.

There are several recent studies on the flow instability under low power conditions. Lee and Ishii (1990) found that non-equilibrium conditions existed between the phases and flashing created flow instability in the loop under low power conditions. Aritomi et al. (1992) observed three kinds of instabilities during the power raising process of a two-phase natural circulation loop with twin boiling channels, such as geysering, in-phase oscillation and out-of-phase density-wave oscillations. Kyung and Lee (1994) investigated the flow characteristics in an open two-phase natural circulation loop using Freon-113 as test fluid. They observed three different modes of oscillation with increase in heat flux such as

(i) periodic oscillation characterized by flow oscillations with an incubation period,
(ii) continuous circulation which is maintained with the churn/wispy-annular flow pattern. This was found to be a stable operation mode in which the flow was found to increase with increase in heat flux first and then decrease with further increase in heat flux, and
(iii) periodic circulation characterized by flow oscillations with continuous boiling inside the heater section (i.e. there is no incubation period) and void fraction fluctuates from 0.6 to 1.0 repeatedly. In this mode, mean circulation rate was found to decrease with increase in heat flux although the mean void fraction kept on increasing.

Jiang et al. (1995) observed three different kinds of flow instability such as geysering, flashing and Type I density-wave oscillations during start-up of the natural circulation loop. Wu et al. (1996) observed that the flow oscillatory behaviour was dependent on the heating power and inlet subcooling. Depending on the operating conditions, the oscillations can be periodic or chaotic.

Moreover, it is evident from these studies that a lot of experimental data exist for various types of flow instabilities in simple two-phase natural circulation systems. Most instabilities such as flashing, geysering, Type I density-wave instability, Ledinegg type instability, etc. in natural circulation systems are found to occur during low pressure conditions. For model validation, it is important to know how to separate them from each other based on their mechanisms and characteristics.

6. STATIC INSTABILITY OF TWO-PHASE NC LOOPS

Extensive comparison of the characteristic equation for static instability with experimental data has been carried out by Rohatgi and Duffey (1998). Stability maps for natural circulation flow are presented in the phase change number and subcooling number plane (i.e. N_p-N_s plane). The characteristic equation predicts two roots corresponding to the instability at low and high quality. According to them, the boundary of the unstable region closer to the zero-quality line is the precursor of static instability, and represents the transition from the single-phase region to the two-phase region. Based on thermal equilibrium, the limiting solution for the first unstable line is $N_p/N_s = 1$. However, if we include subcooled boiling, the first unstable line will be predicted for $N_p/N_s < 1$. Using the Saha-Zuber (1976) model, the limiting stability line for Peclet number greater 70,000 is given by

$$\frac{N_p}{N_s} = \frac{1}{1 + 38.4/(L/D)} \tag{32}$$

The above equation was found to match well with data for $N_p < 150$ (Rohatgi and Duffey). Based on extensive data, they suggest the first unstable line can be represented by

$$\frac{N_p}{N_s} = 0.7 \tag{33}$$

The second boundary represents the transition from two-phase region to very-high void region. Rohatgi and Duffey also found that the high void stability boundary matches fairly well with that predicted by the detailed perturbation analysis. Based on the available experimental data on density wave instability, Rohatgi and Duffey obtained a best fit line given by

$$\frac{N_p}{N_s} = 3 \tag{34}$$

Thus the unstable region is given by $0.7 < N^* < 3$ where $N^* = N_p/N_s$. It is also found that stable natural circulation flow can be maintained below a critical subcooling number. The same equations are also valid for the static instability of parallel channels.

7. DYNAMIC STABILITY OF TWO-PHASE NC LOOPS

In general, two-phase natural circulation loops exhibit two unstable zones as the power is increased. One of these occurs at a low power just at the boiling inception point (and hence at low quality) and the other at a high power (and hence at high quality). Corresponding to these, there are two stability thresholds; the lower stability threshold is sometimes referred to as the threshold of type-I instability and upper one is referred to as threshold of type-II instability (Fukuda and Kobori (1979)). However, due to the hysteresis effects, the stability thresholds are not unique. Chen et al. (2001) provided some experimental evidence for the hysteresis effect on the threshold of instability. Theoretically Achard et al. (1986) established that islands of instability could occur in the stable zone. Although, the first experimental evidence on the existence of islands of instability was provided by Yadigaroglu and Bergles (1969), to our knowledge, experimental data is lacking.

7.1. Instability due to Boiling Inception (Type-I Instability)

Boiling inception has a significant effect on the loop density and hence the gravitational pressure drop. Fukuda and Kobori (1979) have shown that the gravitational pressure drop in the unheated riser plays a dominant role in Type I instability. The mechanism for this instability has already been explained in the second lecture. The homogeneous equilibrium model can predict the instability as has been shown in case of start-up of AHWR in the last lecture. Boiling inception influences both unstable and stable single-phase natural circulation loops

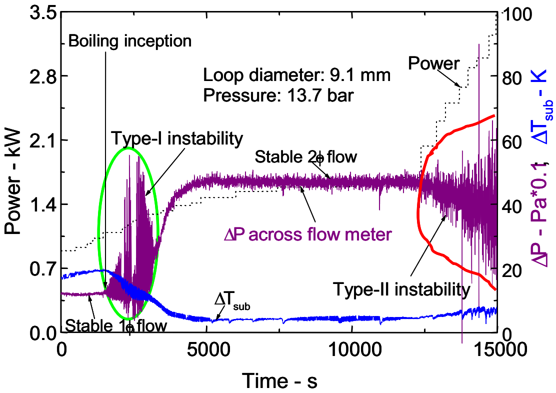

FIG. 26. Typical experimental stability map at 13.7 bar

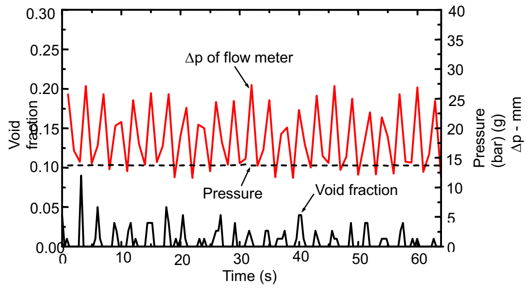

FIG. 27. Instability due to boiling inception

7.1.1. Boiling Inception in an Unstable Single-phase Loop

In this case, the instability continues with part of the oscillation cycle in single-phase flow. Various flow regimes observed with the inception of boiling in an unstable loop were briefly described in the second lecture. Subcooled boiling leads to the formation of the cusps in the phase trajectory (compare Fig. 22a and d). The main reason for the instability is the jump in flow rate occurring during phase change and the accompanying reduction in the exit enthalpy that cannot support two-phase flow.

7.1.2. Boiling Inception in a Stable Single-phase Loop

A stable single-phase system can become unstable due to the inception of boiling as shown in Fig. 26. This instability is important during the start-up of natural circulation BWRs. A basic characteristic of this instability is that single-phase conditions occur in the loop during a part of the oscillation cycle as shown in Fig. 27. Flashing induced instability and geysering also belong to this category. The amplitude of oscillations is found to decrease with increase in pressure. A general characteristic of all instabilities associated with boiling inception is that these are not observed beyond a critical value of the system pressure (Fig.28). The critical pressure beyond which the instability disappears is found to be a function of loop diameter (Compare Figs. 28 and 29).

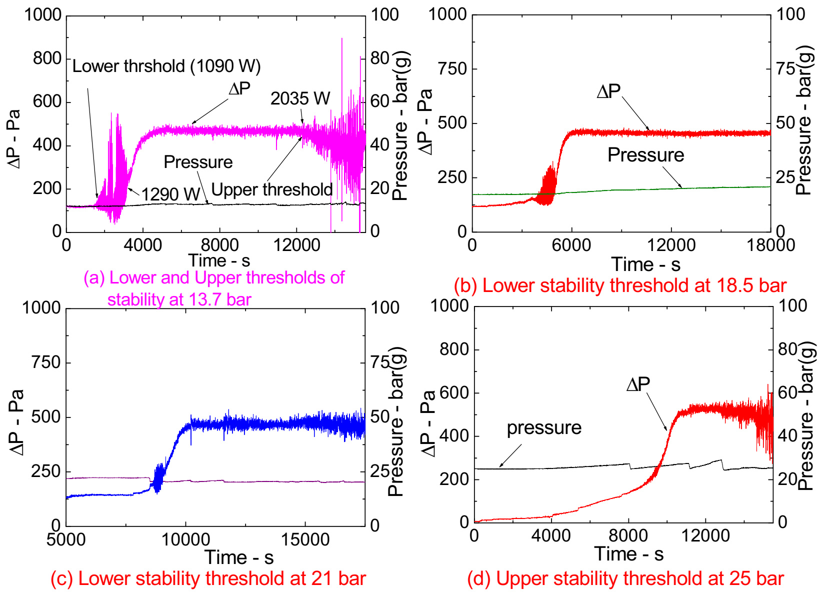

FIG. 28. Effect of pressure on the instability due to boiling inception in 9.6 mm loop

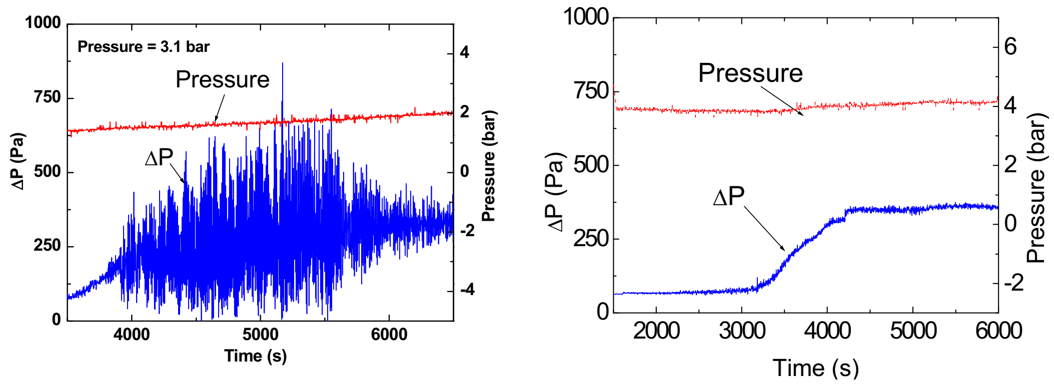

(a) Start-up at 3.1 bar *(b) Start-up at 5.4 bar*

FIG. 29. Effect of pressure on the instability due to boiling inception in 19.2 mm i.d. loop

7.2. Limit Cycles

Unidirectional oscillations are more often observed in two-phase loops with vertical heaters (Fig. 30a). However, bi-directional pulsing and chaotic switching could be observed in loops with horizontal heaters. A Typical limit cycle observed for unidirectional oscillations is given in Fig. 30b. It is found to be similar to that observed in single-phase loops (Fig 17b) except that it is more chaotic. However, the dynamics of the type-I instability is very rich showing several oscillatory modes (Fig. 31).

Non-linear analyses can be used to generate limit cycles of density-wave oscillations (Gurugenci et al. (1983), Chatoorgoon (1986) and Nigamutlin et al. (1993)). Nigamutlin et al. found that the heat transfer coefficient does not affect the threshold of stability while the wall thermal inertia has a strong stabilising effect. Non-linear analyses also revealed the presence of chaotic oscillations in two-phase flow systems (Achard et al. (1986), Rizwaan-Uddin (1990), Lin and Pan (1994)). However, there are very few studies on validation of numerical codes for limit cycle oscillations.

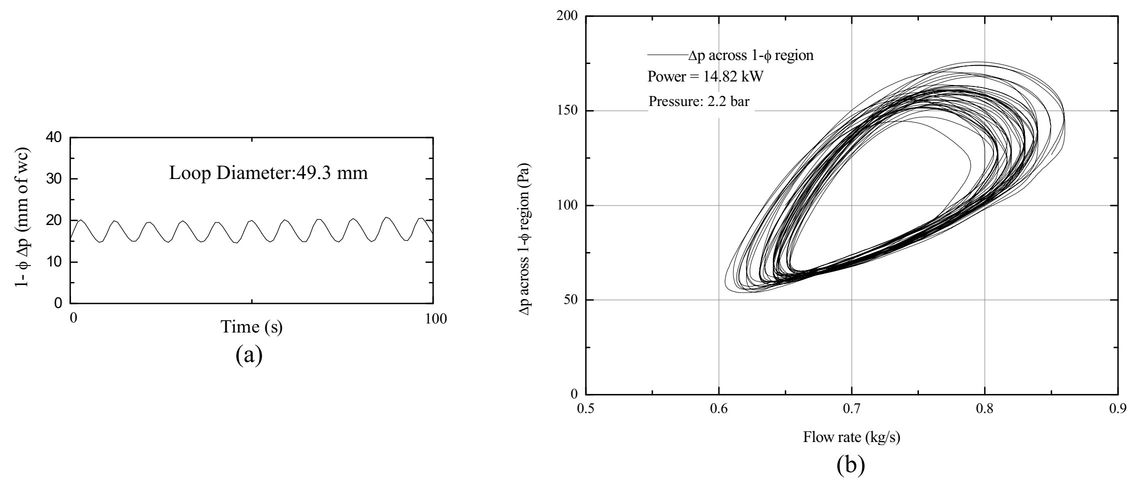

Fig. 30: Time series and Phase plot of type-I instability

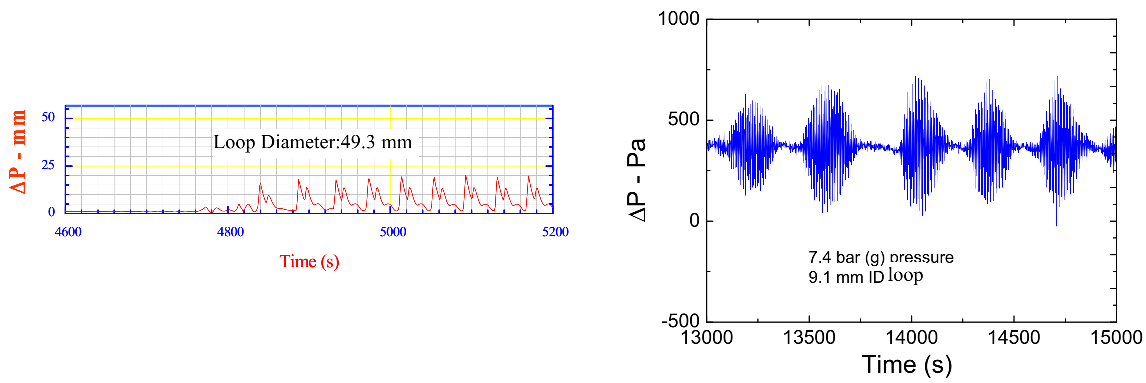

Fig. 31: Different oscillatory modes observed during type-I instability

7.3. Characteristics of Type II instability

Two-phase systems are observed to be stable between a lower and an upper threshold as already explained. The unstable region beyond the upper threshold is known as type II instability (see Fig. 26). Calculations by Fukuda and Kobori (1979) showed that the frictional pressure drop is dominant in type II instability. The upper instability threshold (type-II instability) occurs at high quality and can be predicted by the homogeneous equilibrium model. Experimental data on the occurrence of the upper threshold is shown in Fig. 32 at different pressures. In general, type II instability is observed when the system flow rate begins to reduce with increase in power (friction dominant regime). The amplitude of type-II oscillations increases with increase in power. Calculations for uniform diameter loops show that the type-II instability does not occur in the two-phase region ($0<x<1$) for large diameter loops for 7 MPa pressure. Premature occurrence of CHF is a concern during type-II oscillations especially in small diameter loops. The instability is observed more often at low pressures and occurs at high powers (larger than the critical power) in large diameter loops.

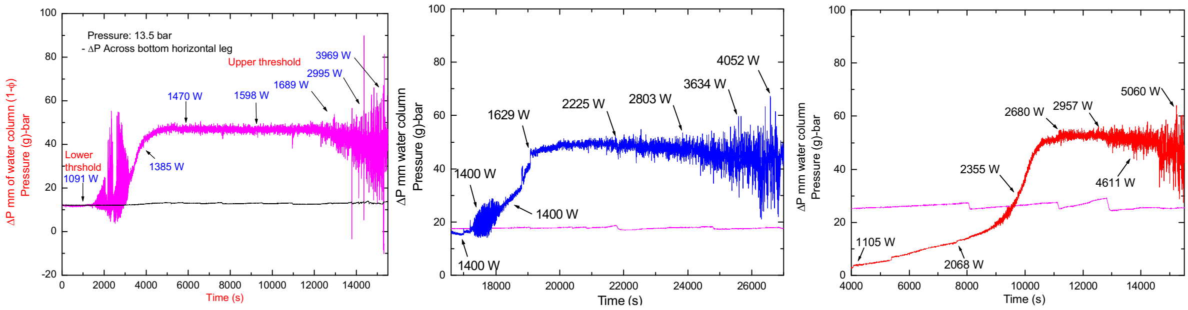

(a) 13.7 bar

FIG..32. The upper threshold of instability at different pressures

7.4. Prediction of Stability Map

Several studies based on linear and non-linear analyses have already been carried out in the past to validate the two-phase flow models for prediction of the threshold of instability. Ishii and Zuber (1970) developed a linear analytical model based on a drift flux model for a two-phase natural circulation loop and plotted the stability maps on non-dimensional parameters. Saha and Zuber (1978) modified Ishii and Zuber's model by taking into account the thermal non-equilibrium effect between the phases. They found that the thermal non-equilibrium effect predicts a more stable system at low subcooling when compared with the thermal equilibrium model. However, their predictions when compared with experiments for the threshold of stability showed poor agreement for high subcooling conditions. Furutera (1986) was probably the first to report the dependence of the threshold of instability on the two-phase friction factor multiplier model and the heat capacity in the subcooled boiling region. Moreover, they showed that the threshold of instability could be predicted with reasonable accuracy using the homogeneous model. Since that many others (Lee and Lee (1991), Wang et al. (1994a &b), Nayak et al. (1998), Van Bragt and Van der Hagen (1998)) showed that it is possible to predict the threshold of instability for density-wave instabilities in two-phase natural circulation systems using the HEM.

However, the applicability of the HEM for prediction of stability threshold still is debatable. Strictly speaking, two fluid model is the ideal one to take care of kinematic and thermodynamic nonequilibrium. However, solution of these balance equations require the models of constitutive relations for interfacial and wall transfer laws which are not well established and are being continuously upgraded. Further, solution of so many equations which are highly non-linear in nature is extremely difficult by the linearised analytical model. An alternative to the two-fluid approach is the drift flux model which replaces the two momentum equations for the liquid and vapour by one momentum equation for the mixture plus a non-differential constitutive law for the relative velocity. So far as the phasic temperature is concerned, one can assume either the thermal equilibrium or thermal nonequilibrium between the phases. Employment of a drift flux model is more realistic than the pure homogenous model. But this needs well assessed models for the drift velocity which is mostly dependent on the flow patterns. It is well known that an increase in drift velocity which is an indication of the slip between the phases reduces the void fraction and hence increase the mixture density. This can increase the gravitational and reduce the frictional component of two-phase pressure drop. At the same time, an increase in drift velocity also reduces the transportation time lag for the fluid to pass through the system. Hence, they can significantly affect the stability.

Aritomi et al. (1983) found that the effect of slip between the phases is to stabilize the flow, since the fluctuation of density reduces with increase in slip for low quality conditions. Fukuda et al. analysed the effect of slip on Type I and Type II density-wave instabilities. They found that the Type I instability stabilizes but the Type II instability destabilizes with inclusion of slip in the model. Since the Type I instability occurs under low quality conditions, the fluctuation of gravitational component of pressure loss can be reduced by slip between the phases which stabilizes the flow. But Ishii and Zuber found an opposite effect to the above for Type II instability. They found that with inclusion of slip, the Type II instability stabilizes due to decrease of pressure drop with increase in slip. A similar result was found by Peng et al. (1984) and Rizwaan-Uddin and Dorning (1986) who found that with increase in slip the flow stabilizes.

Moreover from these studies it can be understood that the slip has a tremendous effect on flow stability. A systematic research must be carried out to understand their effects on the Type I and Type II instabilities. However, mostly the homogenous model is found to be conservative in estimating the stability boundaries, which are good approximations for design purposes of natural circulation systems (Fig. 32).

8. CONCLUDING REMARKS

A brief review of the steady state and stability data obtained from simple loop facilities have been carried out. Data from simple loops were useful to develop the scaling relationships for single-phase flow. Although, large database exists for two-phase flow, due to the lack of generalized dimensionless groups, it is not possible to compare the performance of different loops. It is possible to express the steady state two-phase NC flow in terms of a single dimensionless group for special cases. Phenomenological studies indicate that several unstable flow regimes are possible for both single-phase and two-phase NCSs. Hysteresis phenomenon also exists in both single-phase and two-phase loops. Comparison of stability data shows that the friction pressure drop correlation plays a significant role in case of single-phase loops. Neglecting the heat losses and wall effects, even the same friction factor correlation that gives good steady state results is found to perform poorly while predicting the stability data. For predicting the stability thresholds, it is required to consider the heat transfer to the wall and the heat losses. Although, a pathological friction factor correlation, can give good prediction of the stability threshold, it is not expected to give good prediction of the limit cycles while simulating the unstable flows. For single-phase unstable flows, although, the predicted time series appears similar, the frequency and the shape of the limit cycle are found to be significantly different from the experimental value. Simulation of unstable flows with repetitive flow reversals is a complex problem, since the flow can experience laminar, transition and turbulent regimes repetitively. Besides the flow is never fully developed and 3-D effects are significant. For this case unsteady 3-D nonlinear analysis may be the right choice.

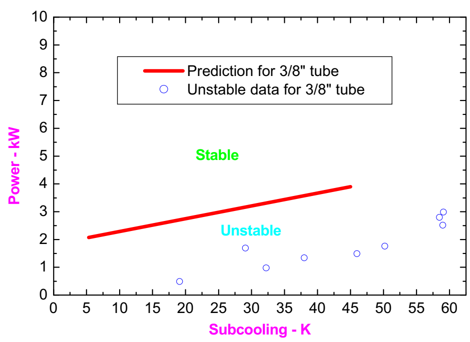

(a) Effect of subcooling at 1 bar

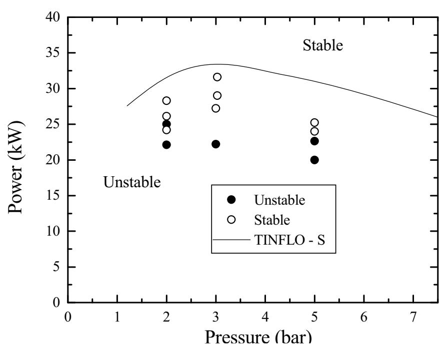

(b) Effect of pressure at 2.5^{0}C subcooling

FIG. 32. Comparison of measured and predicted stability maps

Although, extensive database exists for instability of two-phase loops, often it is not possible to identify the instability type from the data. Both the steady state and the stability threshold of two-phase NCSs can be predicted with reasonable accuracy using the HEM with selected two-phase friction factor multiplier correlations. Extensive validation of the nonlinear codes for the prediction of limit cycle oscillations does not exist. Complete understanding of the occurrence of hysteresis phenomena and islands of stability (or instability) in two-phase NCSs are lacking which are needed for the validation of the computer codes for nonlinear analysis.

NOMENCLATURE

A - flow area, m^2
a_i - dimensionless flow area, A_i/A_r
b - constant in friction factor equation
Cp - specific heat, J/kgK
D - hydraulic diameter, m
d_i - dimensionless hydraulic diameter, D_i/D_r
f - Darcy-Weisbach friction coefficient
g - gravitational acceleration, m/s^2
Gr_m - modified Grashof number, $D^3\rho^2\beta g\Delta T_r/\mu^2$
h - enthalpy J/kg
h_{fg} - latent heat of vaporization, J/kg
H - loop height, m
K - local pressure loss coefficient
k - thermal conductivity, W/mK
l_i - dimensionless length, L_i/L_t
L - length, m
N - total number of pipe segments
N_f - Froude number, $gLA\rho_f^2/W^2$
N_{fr} - friction number, $fL/2D$
N_p - phase change number, $Q_h\rho_f/(Wh_{fg}\rho_g)$
N_{pch} - phase change number (Q_h/Wh_{fg})
N_{sub} - subcooling number $(\Delta h_{sub}/h_{fg})$
N_s - subcooling number, $\Delta h_i\rho_f/h_{fg}\rho_g$
Nu_m - modified Nusselt number, U_iL_t/k
N_G - geometric contribution to the friction number
p - constant in the friction factor equation
Pr - Prandtl number, $Cp\mu/k$
Q_h - total heat input rate, W
Re - Reynolds number, $DW/A\mu$
S - dimensionless co-ordinate around the loop, s/H
s - co-ordinate around the loop, m
St_m - modified Stanton number, $4Nu_m/Re_{ss}Pr$
t - time, s
T - temperature, K
ΔT_r - reference temperature difference $(Q_hH/A\mu Cp)$, K
v - specific volume, m^3/kg
v_{fg} - $v_g - v_f$, m^3/kg
W - mass flow rate, kg/s

Δz - centre line elevation difference between cooler and heater, m

Greek Symbols

β - thermal expansion coefficient, K^{-1}
μ - dynamic viscosity, Ns/m^2
ρ_0 - reference density, kg/m^3
τ - nondimensional time, and residence time, s
ϕ - dimensionless circulation length, L_t/H
ϕ_{LO}^2 - two-phase friction multiplier
ω - dimensionless mass flow rate

Subscripts

c - cooler,
cl - cold leg
d - downcomer
e - equivalent
eff - effective
f - saturated liquid
g - saturated vapour
h - heater
hl - hot leg
i - i^{th} segment
in - inlet
r - reference value
sp - single-phase
ss - steady state
sub - subcooling
t - total
tp - two-phase

Superscripts

$\bar{}$ - average

REFERENCES

Achard, J-L, Drew, D.A, Laher Jr, R.T, 1985, The analysis of nonlinear density wave oscillations in boiling channels, *Journal of Fluid Mechanics,* **155**, pp.213-232.

Ambrosini, W, Forgione, N, Ferreri, J.C, and Bucci, M, The effect of wall friction in single-phase natural circulation stability at the transition between laminar and turbulent flow, to appear in *Annals of Nuclear Energy*, 2004.

Aritomi, M., Chiang, J.H., Nakahashi, T.M., Wataru, M., Mori, M., 1992, Fundamental study on thermohydraulics during start-up in a natural circulation Boiling Water Reactor (I), Thermohydraulic Instabilities, *J. Nucl. Sci. Technol*., **29**, pp.631-640.

Aritomi, M., Aoki, S., Inoue, A., 1983, Instabilities in parallel channels of forced convection boiling upflow system, *J. Nucl. Sci. Technol*., **20**, pp.286-301.

Bau, H.H. and Torrance, K.E., 1981, Transient and steady state behaviour of an open, symmetrically heated, free convection loop, *Int. J. Heat Mass Transfer,* **24**, pp.597-609.

Bernier, M.A. and Baliga, B.R., 1992, A 1-D/2-D model and experimental results for a closed-loop thermosyphon with vertical heat transfer sections, *Int. J. Heat Mass Transfer* **35**, pp.2969-2982.

Chato, J.C., 1963, Natural convection flows in a parallel channel system, *J. Heat Transfer,* **85**, pp.339-345.

Chatoorgoon, V., 1983, SPORTS - A simple non-linear thermal hydraulic stability code, *Nucl. Eng. Des*., vol.. **93**, pp.51-67.

Chen, W.L, Wang, S.B, Twu, S.S, Chung, C.R. and Chin Pan, 2001, Hysteresis effect in a double channel natural circulation loop, *International Journal of Multiphase Flow***,** **27**, 171-187.

Chexal, V.K., Bergles, A.E., 1973, Two-phase flow instabilities in a low pressure natural circulation loop, *AIChE Symposium Series*, **69**, pp.37-45.

Clausse, A., Lahey, R.T., Jr., Podowski, M., 1987, An analysis of stability and oscillation modes in boiling multichannel loops using parameter perturbation methods, *Int. J. Heat Mass Transfer*, **32**, pp.2055-2064.

Creveling, H.F. De Paz, J.F. Baladi, J.Y. and Schoenhals, R.J., 1975, Stability characteristics of a single-phase free convection loop, *J. Fluid Mech.* **67**, 65-84.

Dimmick, G.R, Chatoorgoon, V, Khartabil, H.F. and Duffey, R.B., 2002, Natural convection studies for advanced CANDU reactor concepts, *Nuclear Engineering and Design,* **215**, pp.27-38.

Duffey, R.B., 2000, Natural convection and natural circulation flow and limits in advanced reactor concepts, *IAEA-TECDOC-1281*, pp.49-65.

Fichera, A. and Pagano A., 2003, Modelling and control of rectangular natural circulation loops, *International Journal of Heat and Mass Transfer* **46**, pp.2425-2444.

Fukuda, K., Kobori, T., 1979, Classification of two-phase flow stability by density-wave oscillation model, *J. Nucl. Sci. Technol*., **16**, pp.95-103.

Fukuda, K., Hasegawa, S., 1979, Analysis of two-phase flow instability in parallel multi channels, *J. Nucl. Sci. Technol*., **16**, pp.190-199.

Fukuda, K., Rao, Y.F., Hasegawa, S., Nakagawa, K., Kage, K., 1994, Study on two-phase flow instability in parallel multi channels, *Heat Transfer, Japanese Research*, **23**, pp.693-709.

Furutera, M., 1986, Validity of homogeneous flow model for instability analysis", *Nucl. Eng. Des.,* **95**, pp.65-74.

Gartia, M.R., Vijayan, P.K. and Pilkhwal, D.S. 2006, A Generalized Flow Correlation for Two-Phase Natural Circulation Loops, *Nuclear Engineering and Design*, **236**, pp. 1800-1809.

Gorman, M, Widmann P.J. and Robbins, K.A, 1986, Nonlinear dynamics of a convection loop: a quantitative comparison of experiment with theory, *Physica D* **19**, pp.255-267.

Gurugenci, H., Veziroglu, T.N., Kakac, S., 1983, simplified non-linear descriptions of two-phase flow instabilities in vertical boiling channel, *Int. J. Heat Mass Transfer*, **26**, pp.671-679.

Hallinan, K.P. and Viskanta, R. Heat Transfer from a rod bundle under natural circulation conditions, NUREG/CR-4556.

Haware, S.K. Grover, R.B. and Venkat Raj, V., 1983, Experimental investigation into natural convection heat transfer in an open-loop thermosyphon with horizontal tubes, HMT-D2-83, *Proc. VIIth National Heat and Mass Transfer Conference*, Kharagpur, India.

Ho, C.J, Chiou, S.P. and Hu, C.S, 1997, Heat transfer characteristics of a rectangular natural circulation loop containing water near its density extreme, *Int. J. Heat Mass Transfer,* **40**, pp.3553-3558.

Holman J.P and Boggs, J.H., 1960, Heat transfer to freon 12 near the critical state in a natural circulation loop, *J. Heat Transfer,* **82**, pp.221-226.

Huang, B.J. and Zelaya R., 1988, Heat trans-fer behaviour of a rectangular thermosyphon loop, *J. Heat Transfer* **110**, pp.487-493.

Ishii, M., Zuber, N., 1970, Thermally induced flow instabilities in two-phase mixtures, *4th International Heat Transfer Conference*, Paris.

Jain, K.C., Petric, M., Miller, D., Bankoff, S.G., 1966, Self-sustained hydrodynamic oscillations in a natural-circulation boiling water loop. *Nuclear Engineering and Design,* **4**, pp.233-252.

Jeuck III, P., Lennert and Kiang, R.L., 1981, Single-phase natural circulation experiments on small-break accident heat removal, EPRI-NP-2006.

Jiang, Y.Y. Shoji, M. and Naruse, M., 2002, Boundary condition effects on the flow stability in a toroidal thermosyphon, *International Journal of Heat and fluid flow,* **23** pp.81-91.

Jiang S.Y., Yao, M.S., Bo, J.H., Wu, S.R., 1995, Experimental simulation study on start-up of the 5 MW nuclear heating reactor, *Nucl. Eng. Des*., **158**, pp.111-123.

John, B. and Kannan Iyer, 1991, *Proceedings of 24th National Fluid Mechanics Conference, 1991.*

Kapitaniak, T, 2000, *Chaos for engineers, theory, applications and control*, p 69-86, 2nd revised edition, Springer - Verlag, Berlin.

Keller, J.B., 1966, Periodic oscillations in a model of thermal convection, *J. Fluid Mech.* **26**, pp.599-606.

Kyung, I.S., Lee, S.Y., 1994, Experimental observations on flow characteristics in an open two-phase natural circulation loop, *Nucl. Eng. Des*., **150**, pp.163-176.

Lee, S.Y., Ishii, M., 1990, Characteristics of two-phase natural circulation in Freon-113 boiling loop, *Nucl. Eng. Des.,* **121**, pp.69-81.

Lee, S.Y., Lee, D.W., 1991, Linear analysis of flow instabilities in an open two-phase natural circulation loop, *Nucl. Eng. Des*., **128**, pp.317-330.

Lewis E.E., 1977, *Nuclear Power Reactor Safety*, John Wiley and Sons, New York.

Lin, Y.N., Pan Chin, 1994, Non-linear analysis for a natural circulation boiling channel, *Nucl. Eng. Des*., **152**, pp.349-360.

Loomis, G.G. and Soda, K, 1982, Results of the Semiscale Mod-2A natural-circulation experiments, NUREG/CR-2335, EGG-2200, Idaho National Engineering Lab., Idaho Falls (USA).

Mathisen, R.P., 1967, Out of pile instability in the loop Skalvan, Symp. on Two-phase Flow Dynamics, EURATON, EUR 4288e, vol. 1, 19-64.

Misale, M. Tagliafico, L. and Tanda, G., 1991, Experiments in a free convection rectangular loop, *Proceedings of the fourth International Symposium on Transport phenomena in heat and mass transfer,* Sydney (Australia), 14-19 July, pp.203-211.

Misale, M, Frogheri, M and Ruffino, P, 1998, Steady-state and stability behaviour of a single-phase natural circulation loop, Heat Transfer 1998, *Proceedings of 11th IHTC,* Kyongju, Korea, August 23-28, vol. 3.

Misale, M, and Frogheri, M, 1999, Influence of pressure drops on the behaviour of a single-phase natural circulation loop: Preliminary results, *Int. Comm. Heat Transfer,* **26**, pp.597-606.

Misale, M. Ruffino, P. Frogheri, M., 2000, The influence of the wall thermal capacity and axial conduction over a single-phase natural circulation loop: 2-D numerical study, *Heat and Mass Transfer,* **36**, pp.533 - 539

M. Misale, P. Garibaldi, J.C. Passos, G. Ghisi de Bitencourt, 2007, Experiments in a single-phase natural circulation mini-loop, Experimental Thermal and Fluid Science 31, 1111-1120.

Mousavian, S. K. Misale, M. D'Auria, F. and Salehi, M. A. 2004, Transient and stability analysis in single-phase natural circulation, Annals of Nuclear Energy 31, 1177–1198.

Nayak, A.K, Vijayan, P.K, Saha, D, Venkat Raj, V. and Aritomi M, 1998, Linear analysis of thermo-hydraulic instabilities of the Advanced Heavy Water Reactor (AHWR), *Journal of Nuclear Science and Technology,* **35**, pp.768-778.

Nayak, A.K., Kumar, N., Vijayan, P.K., Saha, D., and Sinha, R.K. 2002, Analytical study of flow instability behaviour of a boiling two-phase natural circulation loop under low quality conditions, KERNTECHNIK 67, pp.95-101.

Nigamutlin, B.I., Melikov, O.I., Blinkov, V.N., Gakal, P.G., 1993, The numerical analysis of boiling flow instabilities in parallel heated channels, *Nucl. Eng. Des.,* **139**, pp.235-243.

Nishihara, T., 1997, Oscillatory instability of a single-phase natural circulation loop, *NURETH-8*, Kyoto, Sept. 30-Oct. 4, pp.839-847.

Peng, S.J., Podowski, M.Z., Lahey, R.T., Becker, M., 1984, A computer code for the stability analysis of Boiling Water reactors, *Nucl. Sci. Eng*., **88**, pp.404-411.

Rizwan-Uddin, Dorning, J.J., 1986, Some non-linear dynamics of a heated channel, *Nucl. Sci. Eng*., **93**, pp.1-14.

Rizwan-Uddin, Dorning, J.J., 1990, Chaotic dynamics of a triply forced two-phase flow system, *Nucl. Sci. Eng*., **105**, pp.123.

Rohatgi, U.S. and Duffey, R.B., 1998) Stability, DNB, and CHF in natural circulation two-phase flow, *Int. Comm. Heat Mass Transfer,* **25**, pp.161-174.

Saha, P., Zuber, N., 1978, An analytical study of the thermally induced two-phase flow instabilities including the effects of thermal non-equilibrium, *Int. J. Heat Mass Transfer*, vol. **21**, pp.415-426.

Satoh, A, Okamoto, K. and Madarame, H., 1998, Instability of single-phase natural circulation under double loop system, *Chaos, Solitons & Fractals,* **9**, 1575-1585.

Satou, A, Madarame, H, Okamoto, K., 2001, Unstable behaviour of single-phase natural circulation under closed loop with connecting tube, *Experimental Thermal and Fluid Science* **25**, pp.429-435.

Todreas, N.E and Kazimi, M.S., 1990, *Nuclear Systems II, Elements of Thermal Hydraulic Design*, Hemisphere Publications, New York, USA.

Van Bragt, D.D.B., Van Der Hagen, T.H.J.J., 1998, Stability of natural circulation Boiling Water Reactors: part I - description stability model and theoretical analysis in terms of dimensionless groups, *Nucl. Technol*, **121**, pp.40-51.

Vijayan, P.K., 1988, Investigations on the single-phase thermosyphon phenomenon in a figure-of-eight loop relevant to pressurized heavy water reactors, *Ph. D. thesis,* Indian Institute of Technology, Bombay.

Vijayan P.K. and Date, A.W., 1992, 'The limits of conditional stability for single-phase natural circulation with throughflow in a figure-of-eight loop', *Nuclear Engineering and Design,* **136**, pp.361-380.

Vijayan, P.K, Nayak, A.K, Pilkhwal, D.S, Saha, D. and Venkat Raj, V, 1992, Effect of loop diameter on the stability of single-phase natural circulation in rectangular loops, *Proc. 5th Int. Topical Meet. on Reactor Thermalhydraulics,*NURETH-5, Salt Lake City, Vol.1, pp.261-267.

Vijayan, P.K. and Austregesilo, H., 1994, Scaling laws for single-phase natural circulation loops, *Nuclear Engineering and Design* **152**, pp.331-347.

Vijayan, P.K. Austregesilo H. and Teschendorff V. 1995, 'Simulation of the unstable oscillatory behaviour of single-phase natural circulation with repetitive flow reversals in a rectangular loop using the computer code ATHLET', *Nuclear Engineering Design* **155**, pp.623-641.

Vijayan P.K., 2000, Scaling of the steady state and stability behaviour of single and two-phase natural circulation systems, *IAEA-TECDOC-1281*, pp.139-156.

Vijayan, P.K, V.K.Bhojwani, M.H. Bade, M. Sharma, A.K.Nayak, D.Saha and R.K. Sinha, 2001, Investigations on the effect of heater and cooler orientation on the steady state, transient and stability behaviour of single-phase natural circulation in a rectangular loop, BARC/2001/E/034, BARC, Mumbai.

Vijayan, P.K. Sharma, M. Nayak, A.K. Bhojwani, V.K. Bade, M.H. Saha D. and Sinha, R.K, 2002, An operating procedure to avoid unstable operating zones in a single-phase natural circulation loop, *Proceedings of 5th ISHMT-ASME Heat and Mass Transfer Conference,* Kolkata, India, Jan. 3-5, pp. 1297-1302.

Vijayan, P.K. Bhojwani, V.K. Sane, N.K. Saha D. and Sinha, R.K., 2002, Is unstable natural circulation loop always a better heat transport device? *Proceedings of 5th ISHMT-ASME Heat and Mass Transfer Conference,* Kolkata, India, Jan. 3-5, pp. 1291-1296.

Vijayan, P.K., 2002, Experimental observations on the general trends of the steady state and stability behavior of single-phase natural circulation loops, *Nucl. Eng. Des.* **215**, pp.139-152.

Vijayan, P.K., 2002, Experimental observations on the general trends of the steady state and stability behaviour of single-phase natural circulation loops, *Nuclear Engineering and Design,* **215**, pp.139-152.

Vijayan, P.K. Bade[1], M.H. Saha, D. Sinha R.K. and Venkat Raj V., 2004, A Generalized Flow Correlation For Single-Phase Natural Circulation Loops, HMT-2004-C022, *Proceedings of 6th ISHMT-ASME Heat and Mass Transfer Conference*, Kalpakkam, India, Jan. 5-7.

Vijayan, P.K. Sharma M. and Saha, D. 2007, Steady state and stability characteristics of single-phase natural circulation in a rectangular loop with different heater and cooler orientations, *Experimental Thermal and Fluid Science* **31**, 925-945.

Wang, Q., Chen, X.J., Kakac, S., Ding, Y., 1994a, An experimental investigation of density-wave type oscillations in a convective boiling upflow system, *Int. J. Multiphase Flow*, **15**, pp.241-246.

Wang, F.S., Hu, L.W., Pan, C., 1994b, Thermal and stability analysis of a two-phase natural circulation loop*, Nuclear Science and Engineering,* **117**, pp.33-46.

Welander, P., 1967, On the oscillatory instability of a differentially heated loop, *J. Fluid Mech.* **29**, pp.17-30.

Widmann, P.J, Gorman M. and Robbins K.A, 1989, Nonlinear Dynamics of a convection loop II. Chaos in laminar and turbulent flows, *Physica D* **36**, pp.157-166.

Wu, C.Y., Wang, S.B., Chin-Pan, 1996, Chaotic oscillations in a low pressure two-phase natural circulation loop, *Nucl. Eng. Des*., vol. **162**, pp.223-232.

Yadigaroglu, G. and Bergles, A.E., 1969, An experimental and theoretical study of density-wave oscillations in two-phase flow, MIT rept. DSR 74629-3 (HTL 74629-67), 1969.

Zvirin, Y. Jeuck III P, Sullivan, C.W, Duffey, R.B, 1981, Experimental and analytical investigation of a natural circulation system with parallel loops, *J. Heat Transfer* **103**, pp.645-652.